

Precursor Effects and Ferroelectric Macroregions in $\text{KTa}_{1-x}\text{Nb}_x\text{O}_3$ and $\text{K}_{1-y}\text{Li}_y\text{TaO}_3$

J. Toulouse, P. DiAntonio, B. E. Vugmeister, X. M. Wang, and L. A. Knauss

Physics Department, Lehigh University, Bethlehem, Pennsylvania 18015

(Received 11 July 1991)

In the present paper, dielectric, polarization, and Raman results have been combined to identify the existence of a ferroelectric phase transition in the substitutionally disordered dipolar system, $\text{KTa}_{1-x}\text{Nb}_x\text{O}_3$, for low Nb concentrations ($x=1.2\%$). A detailed study of the first-order TO_2 and TO_3 Raman lines reveals (1) the existence of polar microregions well above T_c and (2) the structural transition at T_c with the appearance of ferroelectric macroregions. Similar results are obtained in $\text{K}_{1-y}\text{Li}_y\text{TaO}_3$ with a quantitative difference due to the slow reorientation of Li. These results can be explained by a random-field model which predicts the coexistence of both dipolar glass and ferroelectric behavior.

PACS numbers: 77.80.Bh

The occurrence and nature of phase transitions in mixed ferroelectric systems is an intriguing topic since the introduction of configurational disorder should normally prevent the establishment of long-range order. Among these systems, $\text{KTa}_{1-x}\text{Nb}_x\text{O}_3$ (KTN) and $\text{K}_{1-y}\text{Li}_y\text{TaO}_3$ (KLT) may have been studied the longest. Both are also now probably the systems for which there exists the greatest number of experimental results [1–3]. Yet, after almost thirty years, there still does not exist a general answer to the two most basic questions concerning their behavior at lower concentrations: (1) Do these two systems freeze in a dipolar glass state or do they undergo a ferroelectric phase transition? (2) If a ferroelectric transition does occur, what is its nature as compared to those observed in ordinary ferroelectrics? Over the years, various authors have provided mixed answers to the two questions above. Although the behavior of the two systems is fundamentally the same, we initially focus our attention on KTN, for which the controversy is still very much alive.

In one of the earlier attempts at characterizing the behavior of the mixed ferroelectric KTN, Rytz and Scheele [4] published a phase diagram on which they indicated above 5% Nb three successive transitions similar to those observed in pure ferroelectrics such as KNbO_3 or BaTiO_3 , and below 5% Nb a single ferroelectric transition from a cubic to a rhombohedral phase.

Dielectric results were reported by Samara [5] for 0.9% and 2% Nb. His conclusion was that KTN with small x (≤ 0.02) exhibited a relaxational glasslike behavior rather than a static ferroelectric structural phase transition. In contrast with the 0.9% crystal, however, the 2% Nb crystal did not exhibit any dispersion unless subjected to high pressures. Kleemann, Schafer, and Rytz [6] in a study of 0.8%, 1.2%, and 2% Nb crystals reported refractive index and linear birefringence measurements which they explained on the basis of a “cooperative dipole glass model.” In their model, local ordering within finite Curie regions of a diffuse phase transition was followed by a strain-induced reorientation of frozen microdomains. In a Raman study of normally pure KTaO_3 and KTN with 0.9% Nb, Uwe *et al.* [7] did observe disorder-induced scattering due to microscopic ferroelectric regions, the size of which increased with decreasing

temperature. They suggested that T_c should be associated with the temperature at which these regions overlap. As to the origin of the microscopic regions, they concluded that there was no necessary link to the presence of niobium because similar regions were also observed in their nominally pure sample. Prater, Chase, and Boatner [8] reached a similar conclusion due to the apparent independence of the disorder-induced Raman features on the Nb concentration. This interpretation was in conflict with Yacoby’s conclusion as to the presence of Nb-induced microdistortions [9]. Finally, the incomplete optic-phonon mode softening reported by Chou *et al.* [10] on the basis of inelastic neutron and Raman scattering was used as evidence against a structural transition and in support of the dipolar glass model. More recently, Lyons *et al.* [3] have clearly described the dichotomic behavior of KTN, “on the one hand suggesting the presence of ordered domains of macroscopic extent, and on the other indicating a dynamic cluster behavior.” In order to resolve this dichotomy, they suggested a percolated cluster model for the dipolar glass phase in KTN.

In the present Letter we show that, rather than being antinomic, the two simultaneous behaviors observed in KTN result from the coexistence of the ferroelectric and dipolar glass states, each to varying degrees depending on the Nb concentrations and the presence of structural defects or internal strain. The evidence to support this coexistence model is obtained from comparative dielectric and Raman measurements made on the same 1.2% KTN crystal. The model is further supported by Raman results obtained on 1% and 4% KLT crystals.

In ferroelectrics, the dielectric susceptibility and the polarization constitute the most direct macroscopic probes of the transition. In Fig. 1, we present data for the ac dielectric constant ϵ of two 1.2% Nb crystals, I and II, measured at two different frequencies. Both crystals were grown by Rytz. Crystal I was also previously used in Refs. [11] and [12] and for our own Raman study below. In crystal I, ϵ exhibits a sharp maximum at $T \approx 15.5$ K, decreasing at lower temperatures much more rapidly than what is observed at lower concentrations. The ϵ peak in crystal I is also remarkably high, exceeding 10^5 which constitutes, to our knowledge, a KTN record. More importantly, this peak height is an indication of the

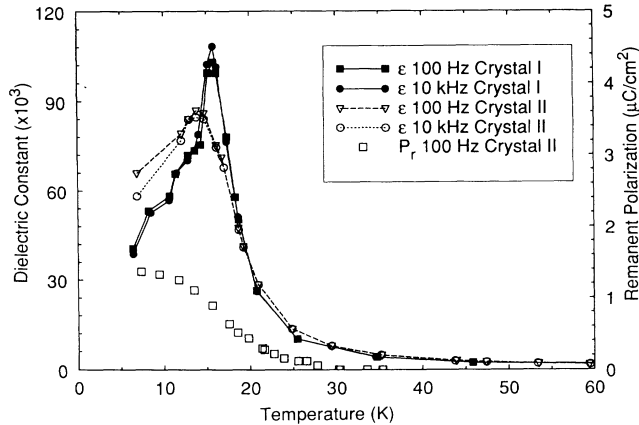


FIG. 1. Dielectric constant of two KTN 1.2% Nb crystals, I and II, as a function of temperature measured at 100 Hz and 10 kHz, and remanent polarization measured with $E_{\max} = 4$ kV/cm at 100 Hz for KTN 1.2% Nb crystal II.

very high quality of the crystal. The ϵ peak for another nominally 1.2% KTN crystal (II) is shown to illustrate the variations that can be observed between samples with approximately the same concentration. The ϵ peak in crystal II is lower than in crystal I, presumably due to the presence of structural defects or internal strain. We have also measured hysteresis loops on crystal II using a Sawyer-Tower circuit with a maximum bias field of 4 kV/cm and a 100-Hz frequency after cooling in zero field. As shown in the lower part of Fig. 1, a nonzero remanent polarization appears at about 30 K and increases with decreasing temperature. These dielectric and polarization results do not strongly support a dipolar glass model but rather favor the existence of long-range ferroelectric order even for $x = 1.2\%$ Nb, i.e., close to the critical niobium concentration, $x_{cr} \approx 0.8\%$. However, we note in Fig. 1 signs of dielectric dispersion below the peak, particularly for crystal II. This dispersion, which becomes stronger at lower Nb concentrations [6], points to the coexistence of a certain degree of orientational disorder with the ferroelectric long-range order.

Decisive arguments in favor of the occurrence of a transition are obtained from a Raman study of the two "hard" optic modes, TO_2 and TO_3 . As is well known, there exist in $KTaO_3$, KTN, and KLT four distinct transverse optic modes TO_1 , TO_2 , TO_3 , and TO_4 [11]. All of them are odd-parity phonons and, as a result, they are not Raman active in the cubic phase. Of these four modes, only TO_3 is a nonpolar mode. In Fig. 2, we present Raman spectra for the TO_2 and TO_3 modes at 10.5, 17, and 33 K. With $T_c \approx 15.5$ K, we see that the TO_2 line appears at 200 cm^{-1} significantly above the transition. It is initially broad and asymmetrical and its appearance, as well as that of the TO_4 line, coincides with the appearance of the remanent polarization. As the temperature decreases, the TO_2 line increases in height and becomes narrower ($\sim 2\text{ cm}^{-1}$). Contrary to the TO_2 line, the TO_3 line appears at about 277 cm^{-1} and its appearance

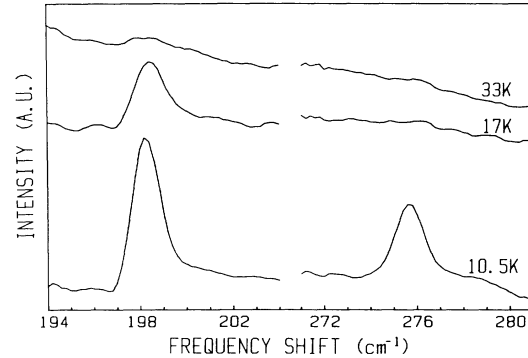


FIG. 2. Raman spectra of the TO_2 and TO_3 modes at 10.5, 17, and 33 K for 1.2% KTN crystal I.

almost coincides with the peak in the dielectric constant. It is relatively narrow and symmetrical in shape. The same two lines are also observed in KLT 4%, appearing in the same order and displaying the same trend as far as width, shape, and intensity are concerned. In Fig. 3, we compare intensities of the TO_2 and TO_3 lines for KTN 1.2% and KLT 1% and 4%. For both KTN 1.2% and KLT 4%, the TO_2 line exhibits a sharp drop at 14.5 and 55 K, respectively, which corresponds to the appearance of the TO_3 line. By contrast, for KLT 1%, the TO_3 line is not observed down to 6 K suggesting that no ferroelectric transition occurs for that low a concentration, in agreement with previous studies [12]. We also note a significant difference in the temperature dependence of the TO_2 line between KTN and KLT. In the former, the TO_2 line appears at a much lower temperature and its intensity rises much faster with decreasing temperature than in the latter.

The main point of the Raman results presented above is the difference in the behavior of the first-order TO_2 and TO_3 lines corresponding respectively to a polar and a nonpolar mode. The assignment of these lines to single-phonon transitions is warranted by their positions and widths, the latter being much less than for the second-order features observed in the spectrum. Because the appearance of the TO_2 line coincides with the observation of the remanent polarization, we can attribute it to the coupling of the light to the polarization of polar microregions or clusters. In stark contrast, the appearance of the TO_3 line cannot be attributed to the same process since it corresponds to a nonpolar mode. Its appearance can then only reflect the onset of a structural distortion extended over a distance of the order of the phonon wavelength. However, the onset of this distortion also coincides with the maximum of the dielectric constant, indicative of a transition with the formation of ferroelectric macroregions. As we have mentioned before when presenting the dielectric results, we emphasize that these macroregions can nevertheless coexist with a certain degree of orientational disorder.

This coexistence can be explained by a model recently proposed [13] in which, in a highly polarizable lattice,

each off-center dopant atom is characterized by an effective dipole moment d^* , each polarizing an extended region of radius $r_c \sim \epsilon_0^{1/2}$. This radius corresponds to the correlation length of the highly polarizable host lattice with dielectric constant ϵ_0 . When r_c becomes greater than the average distance between dipoles, one must define a new radius $R_c = [\epsilon(T)/\epsilon_0]^{1/2} r_c$ in which $\epsilon(T)$ is the dielectric constant of the doped lattice. In order to describe such a random dipolar system, an orientational order parameter L is introduced such that $L = \langle \bar{l}_i \rangle$, where l_i is a unit vector along the dipole located on site i and where the two averages are respectively configurational and ensemble averages. It can be shown [14] that only above a certain critical concentration x_{cr} , for which $T_c = 0$, does the order parameter L become greater than zero and yield complete long-range order.

This model can now be extended to describe the appearance of the first-order Raman TO_2 line above the transition. Changes in the electronic polarizability due to polar optic phonons can be written in the form

$$\delta\alpha(\mathbf{r}, t) = \mathbf{P}(\mathbf{r}, t) \cdot \bar{\Lambda} \cdot \mathbf{P}(\mathbf{r}, t), \quad (1)$$

where $\mathbf{P}(\mathbf{r}, t)$ represents the space- and time-dependent polarization fluctuation and $\bar{\Lambda}$ is a fourth-rank tensor. Equation (1) usually describes second-order Raman scattering; however, if the polarization fluctuation spectrum contains a low-frequency component, such as the slow relaxation modes due to polar microregions, Eq. (1) can describe single-phonon Raman scattering as well. To show this, we write the polarization as a sum over polar hard optic modes and slowly relaxing microregions: $P = \sum (P_h + P_\mu)$.

In order to explain the appearance of single-phonon Raman lines above T_c , we are only concerned in Eq. (1) with cross terms of the form $P_\mu P_h$. The scattered intensity can be written as (see also Ref. [15])

$$I_h(\omega) = \langle \delta\alpha(\mathbf{r}, t) \delta\alpha(0, 0) \rangle \sim \sum \int_{q'} d\omega' \langle P_\mu(\mathbf{r}, t) P_\mu(0, 0) \rangle_{q', \omega'} \langle P_h(\mathbf{r}, t) P_h(0, 0) \rangle_{-q', \omega - \omega'}. \quad (2)$$

Because the first correlation function possesses a sharp maximum near $\omega' = 0$ and the second one near Ω_q , $I(\omega)$ is sharply peaked at $\omega = \Omega_q$, i.e., near the hard single-phonon frequency. We note that this theory is equally applicable to the TO_4 mode and, indeed, its experimentally observed behavior (temperature dependence of the intensity) is similar to that of the TO_2 mode. Also, terms of the form $P_\mu P_\mu$ in Eq. (1) will contribute to the quasi-elastic or central peak scattering also observed by us and others [3,16]. Using the results of Ref. [17] in Eq. (2) for the first correlation function and the "static" limit of slowly relaxing dipoles, we can write $I_h(\omega)$ in the following form:

$$I_h^{st}(\omega) \sim \frac{q_\omega}{(r_c^{-2} + q_\omega^2)(R_c^{-2} + q_\omega^2)} \quad (3)$$

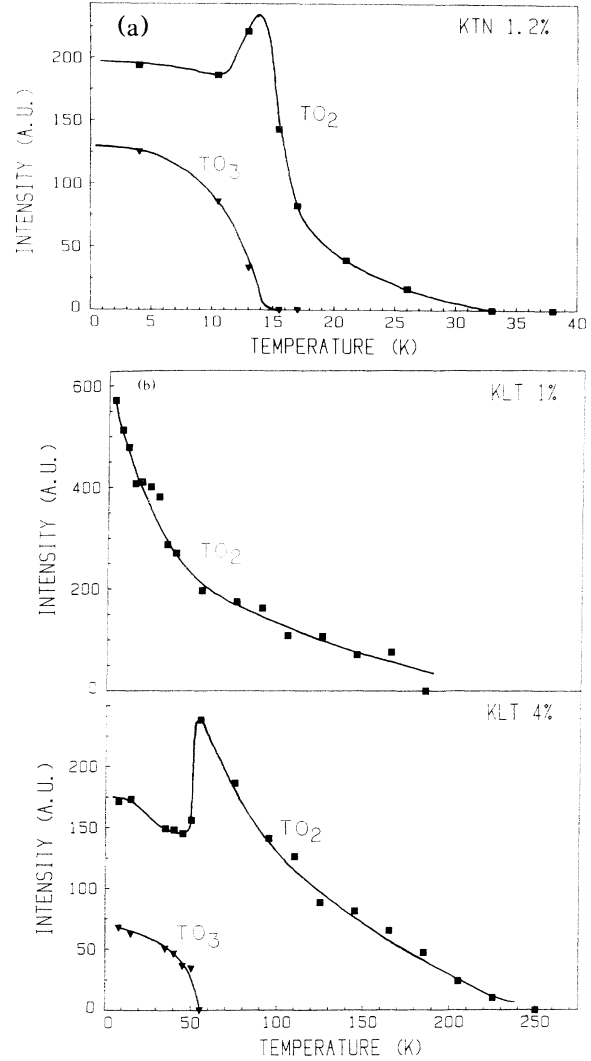


FIG. 3. Raman line intensities of the TO_2 and TO_3 modes as a function of temperature for (a) KTN 1.2% Nb crystal I and (b) KLT 1% and 4% Li.

in which $q_\omega = (\omega^2 - \Omega_0^2)/v^2$, Ω_0 being the hard phonon mode frequency at $q_\omega = 0$ and v its velocity. For $R_c \gg r_c$, $I_h^{st}(\omega)$ is maximum for $q_\omega^2 = R_c^{-2}$, namely, at $\omega_{max}^2 = \Omega_0^2 + R_c^{-2}v^2$ with $I_h^{st}(\omega_{max}) \sim r_c^2 R_c$. The increase in the intensity of the TO_2 line shown in Fig. 3 can be attributed, above T_c , to an increase in R_c with decreasing temperature. Also in the static limit, the width of the line at half maximum is found from Eq. (3) to be $\Delta\omega_{HM} \approx (3\omega_s^2/\Omega_0)\epsilon_0/\epsilon$ in which ω_s is the soft mode frequency. Using the experimental values $\omega_s \sim 20 \text{ cm}^{-1}$, $\Omega_0 \sim 200 \text{ cm}^{-1}$, and $\epsilon_0/\epsilon \sim 0.1$, we get $\Delta\omega_{HM} \sim 1 \text{ cm}^{-1}$ which is close to the observed value ($\sim 2 \text{ cm}^{-1}$). The asymmetrical shape of the TO_2 line is also properly described by the theory.

The static limit in which the above theory has been

presented applies well to the KLT system. Lithium is indeed known to reorient very slowly in the temperature range of interest [18] (≤ 250 K), such that the static limit is appropriate throughout this range. As derived above, $I_{\max}^{\text{st}} \sim r_c^2 R_c = \epsilon_0 \sqrt{\epsilon(T)}$ which yields a moderate temperature dependence as observed. By contrast, the intensity of the TO_2 line in KTN (Fig. 3) exhibits a much stronger temperature dependence than in KLT. We attribute this difference to the existence of a distribution of relaxation times for the niobium atoms. This assumption is quite plausible in KTN since the niobium atoms find themselves in much shallower potential wells than the lithium atoms in KLT [3]; they are consequently more strongly affected by their local environments. As the temperature decreases, an increasing number of Nb atoms contribute to the slow relaxational modes and to $I(\omega)$ by virtue of Eq. (1). For KTN thus, the intensity can be approximately written as

$$I_{\max} = I_{\max}^{\text{st}} \int_0^{v \leq \Delta\omega_{\text{HM}}} \phi(v') dv' \quad (4)$$

in which $\phi(v')$ is the distribution function. The temperature dependence of the last term is contained in the upper limit of integration, e.g., $v = v_0 e^{-U/kT}$, where v_0 is an attempt frequency and U is the activation energy. The preceding explanation is also supported by the simultaneous appearances of the remanent polarization and the first-order TO_2 line. Equation (4) also explains why I_{\max} cannot be simply proportional to the Nb concentration as reported earlier [3,8].

In conclusion, dielectric and Raman measurements, performed on the same crystal, have shown evidence for (1) the formation of precursor clusters or polar microregions many degrees above the transition; (2) the occurrence, even for low concentrations, of a transition corresponding to a structural distortion on the scale of a Raman phonon wavelength and accompanied by the appearance of ferroelectric macroregions; and (3) the coexistence, below the transition, of these macroregions with a certain degree of orientational disorder which explains the observed dipolar glasslike behavior previously reported. We note that this behavior persists to much higher concentrations than those discussed here [19]. Finally the model proposed explains qualitatively the asymmetrical TO_2 line shape and the stronger temperature dependence of the time intensity in KTN relative to KLT. A detailed analysis of this temperature dependence (intensity and linewidth) will be given elsewhere.

ty and linewidth) will be given elsewhere.

This work was partially supported by Office of Naval Research Grant No. N00014-90-J-4098 (P.D.) and by the Division of Materials Sciences, U.S. Department of Energy, under Contract No. DE-FG02-86ER45258 (X.M.W., L.A.K., J.T.). We owe particular thanks to K. B. Lyons and D. Rytz for making the 1.2% crystals available to us.

-
- [1] B. E. Vugmeister and M. D. Glinchuk, *Rev. Mod. Phys.* **62**, 993 (1990).
 - [2] U. T. Hochli, *Adv. Phys.* **39**, (1990).
 - [3] K. B. Lyons, P. A. Fleury, H. Chou, J. Kjems, S. M. Shapiro, and D. Rytz, in *Proceedings of the First U.S.A.-U.S.S.R. Joint Symposium on Ferroelectrics*, July 1989, Boulder, Colorado [Ferroelectrics (to be published)].
 - [4] D. Rytz and H. J. Scheele, *J. Cryst. Growth* **59**, 468 (1982).
 - [5] G. A. Samara, *Phys. Rev. Lett.* **53**, 298 (1984); *Jpn. J. Appl. Phys.* **24**, Suppl. 24-2, 80 (1985).
 - [6] W. Kleemann, F. J. Schafer, and D. Rytz, *Phys. Rev. Lett.* **54**, 2038 (1985).
 - [7] H. Uwe, K. B. Lyons, H. L. Carter, and P. A. Fleury, *Phys. Rev. B* **33**, 6436 (1986).
 - [8] R. L. Prater, L. L. Chase, and L. A. Boatner, *Phys. Rev. B* **23**, 221 (1981).
 - [9] Y. Yacoby, *Z. Phys. B* **31**, 275 (1978).
 - [10] H. Chou, S. M. Shapiro, K. B. Lyons, J. Kjems, and D. Rytz, *Phys. Rev. B* **41**, 7231 (1990).
 - [11] S. K. Manlief and H. Y. Fan, *Phys. Rev. B* **5**, 4046 (1972).
 - [12] W. Kleemann, S. Kutz, and D. Rytz, *Europhys. Lett.* **4**, 239 (1987).
 - [13] B. E. Vugmeister and M. D. Glinchuk, *Zh. Eksp. Teor. Fiz.* **79**, 947 (1980) [*Sov. Phys. JETP* **52**, 482 (1980)].
 - [14] B. E. Vugmeister, *Fiz. Tverd. Tela (Leningrad)* **26**, 2448 (1984) [*Sov. Phys. Solid State* **26**, 1483 (1984)].
 - [15] A. D. Bruce, W. Taylor, and A. F. Murray, *J. Phys. C* **13**, 483 (1980).
 - [16] J. P. Sokoloff, L. L. Chase, and L. A. Boatner, *Phys. Rev. B* **41**, 2398 (1990).
 - [17] B. E. Vugmeister, *Fiz. Tverd. Tela (Leningrad)* **26**, 1080 (1984) [*Sov. Phys. Solid State* **26**, 658 (1984)].
 - [18] V. T. Hochli, H. E. Weibel, and L. A. Boatner, *Phys. Rev. Lett.* **41**, 1440 (1978).
 - [19] J. Toulouse, X. M. Wang, L. A. Knauss, and L. A. Boatner, *Phys. Rev. B* **43**, 8297 (1991).